HRV RECORDING REPORT

ANON-9AD40F75

2026-10-23 17:09:00 (Europe/Berlin) · 47:51 · 5 544 beats

SENSOR	START TIME SOURCE	PARTICIPANT
Polar H10	not recorded	ANON-9AD40F75 (pseudonymised)

Beat quality Excellent — 0.97 % of beats flagged and corrected (54 of 5 544: 20 ectopic · 27 long/short · 7 missed) over 47:51

Beat quality grades only flagged beats: excellent < 1 %, good < 3 %, limited < 10 % flagged beats. Flagged beats are marked in Figure 2. Rhythm check: 0.04 % of the beats with five neighbours on each side show a premature pattern (note from 5 %). The overall measurement_quality score in the JSON also weighs duration, stationarity, protocol and breathing context.

TIME DOMAIN

Mean HR	RMSSD	SDNN	pNN50
115.9 bpm	15.8 ms	88.0 ms	1.9 %
heart rate	beat-to-beat	overall	steps > 50 ms

POINCARÉ & NONLINEAR

SD1	SD2	SD2/SD1	DFA α1
11.2 ms	124.0 ms	11.09	1.41
short-term	long-term	shape ratio	no detrending

FREQUENCY DOMAIN · WELCH

Total power	LF	HF	LF/HF §
1428 ms²	480 ms²	105 ms²	4.55
≤ 0.40 Hz	0.04–0.15 Hz	0.15–0.40 Hz	power ratio

GEOMETRIC & STRESS

TINN	√Baevsky SI	Ectopic	Artefacts
234 ms	12.7 AU	20 beats	0.97 %
histogram base	stress index	classified	flagged

§ Low confidence without a breathing record: slow breathing moves power from HF into LF.
Thresholds after Task Force of the ESC and NASPE (1996).

LIMITATIONS OF THIS RECORDING

- No breathing record: frequency-domain values (LF, HF, LF/HF) cannot be related to breathing rate.
- Whole-recording DFA α1 averages across all phases of the recording; use the α1 time course (Figure 8) and the per-window CSV for interpretation.

TIME SERIES

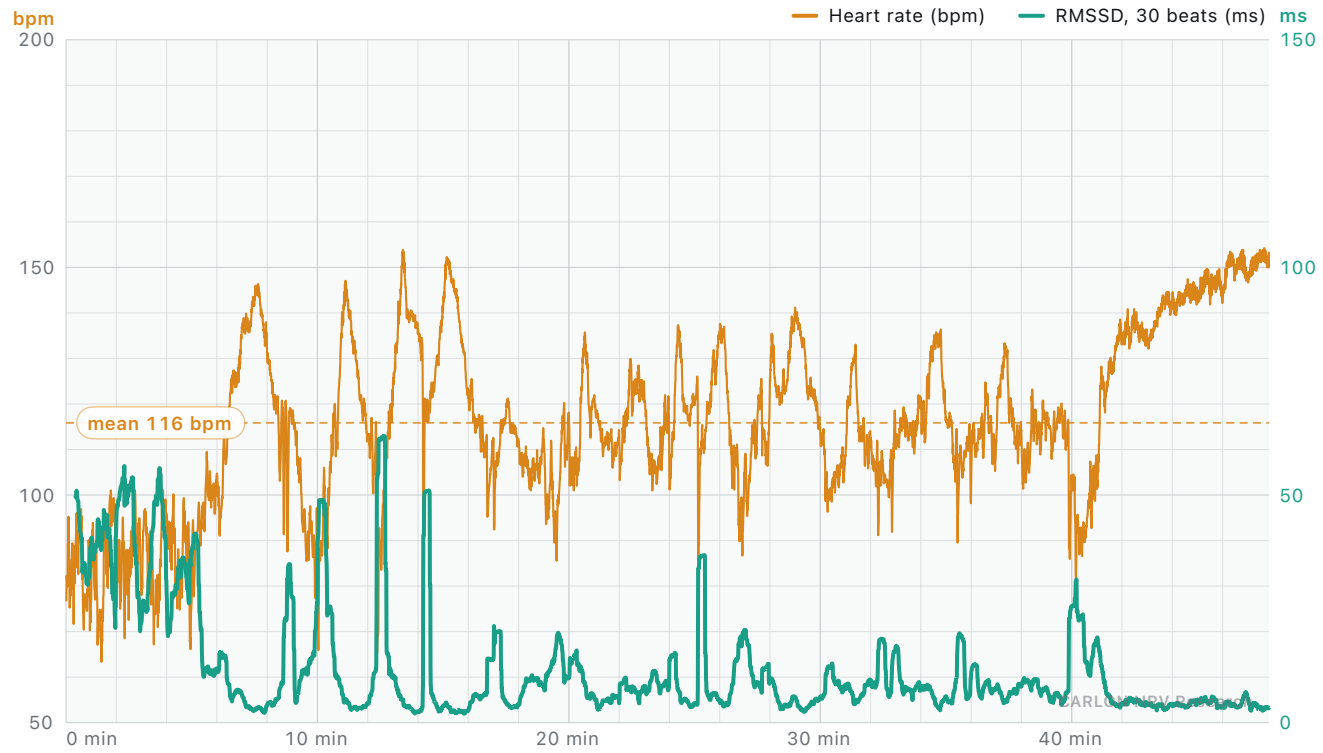


Figure 1. Heart rate per beat (left axis) and RMSSD over a sliding window of 30 beats (right axis). Dashed: mean heart rate (116 bpm).

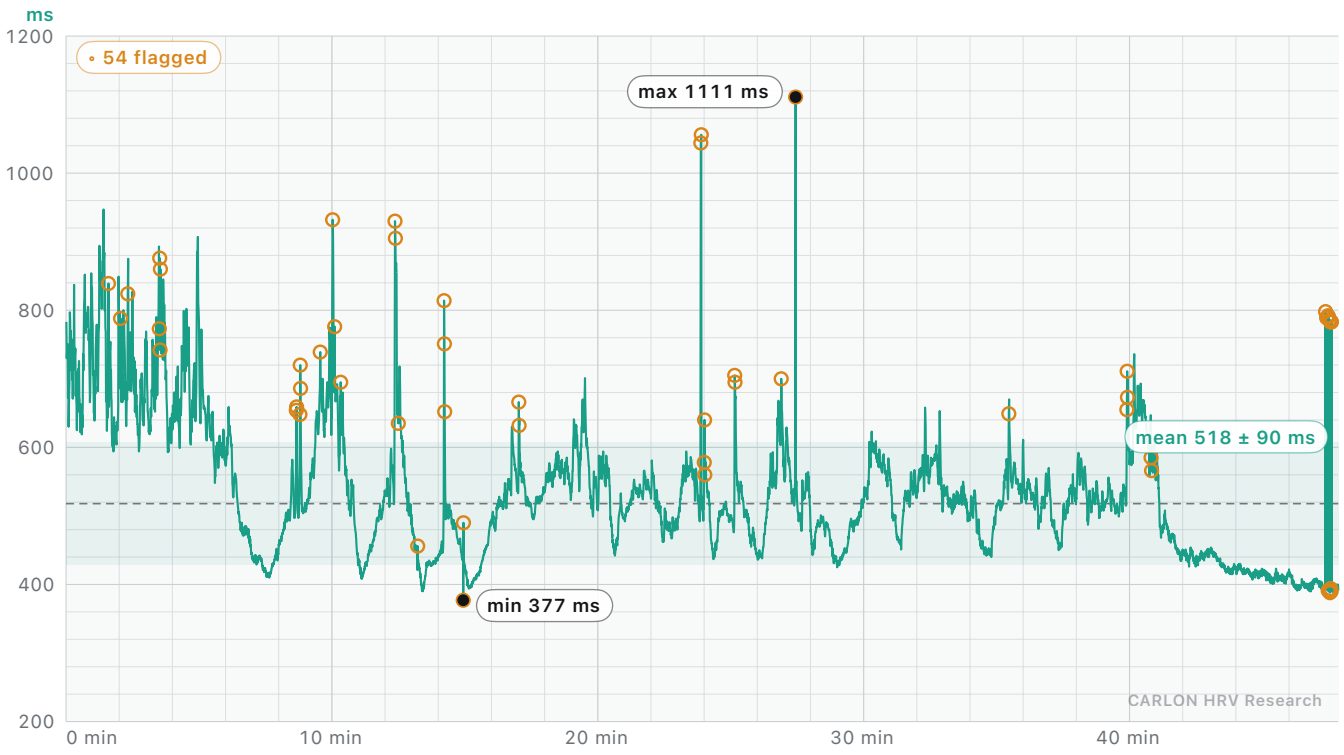
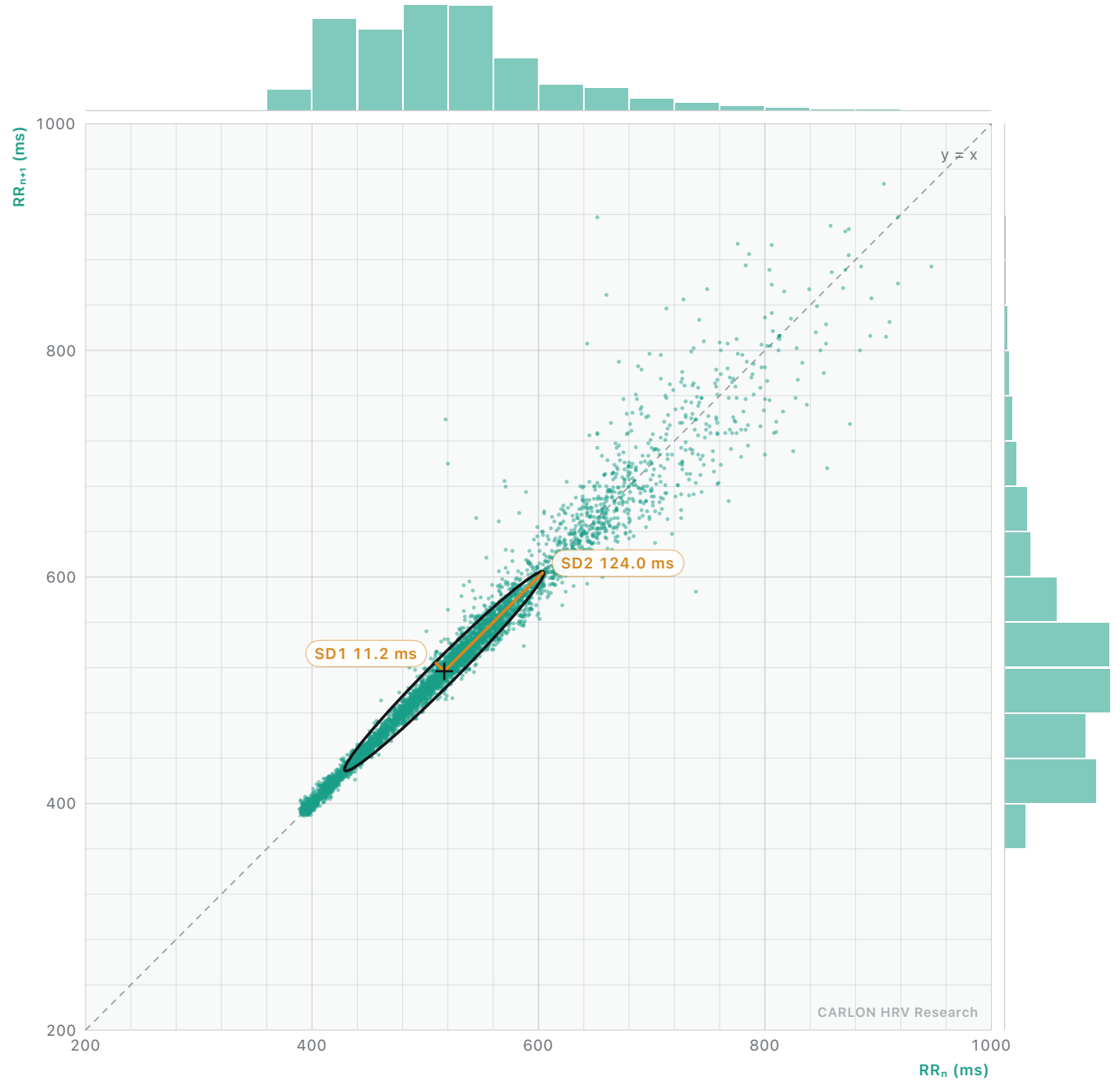


Figure 2. RR tachogram — original intervals as recorded, before artefact correction. Band: mean ± 1 SD (518 ± 90 ms); marked: shortest and longest interval. Amber rings: beats flagged as artefacts (54), shown at their recorded value and corrected in the analysis series (Lipponen & Tarvainen 2019, duration kept).

POINCARÉ ANALYSIS



n pairs	mean RR	SD1	SD2	SD2/SD1	S = π·SD1·SD2
5 554	517 ms	11.2 ms	124.0 ms	11.09	4 356 ms²

Figure 3. Poincaré plot of successive RR pairs (corrected series). Ellipse with semi-axes SD1 (across the identity line, short-term variability) and SD2 (along it, long-term variability), centred on the mean RR (Brennan et al., 2001). Margins: distributions of RR_n (top) and RR_{n+1} (right) in the grid's bin width.

POINCARÉ OVER TIME

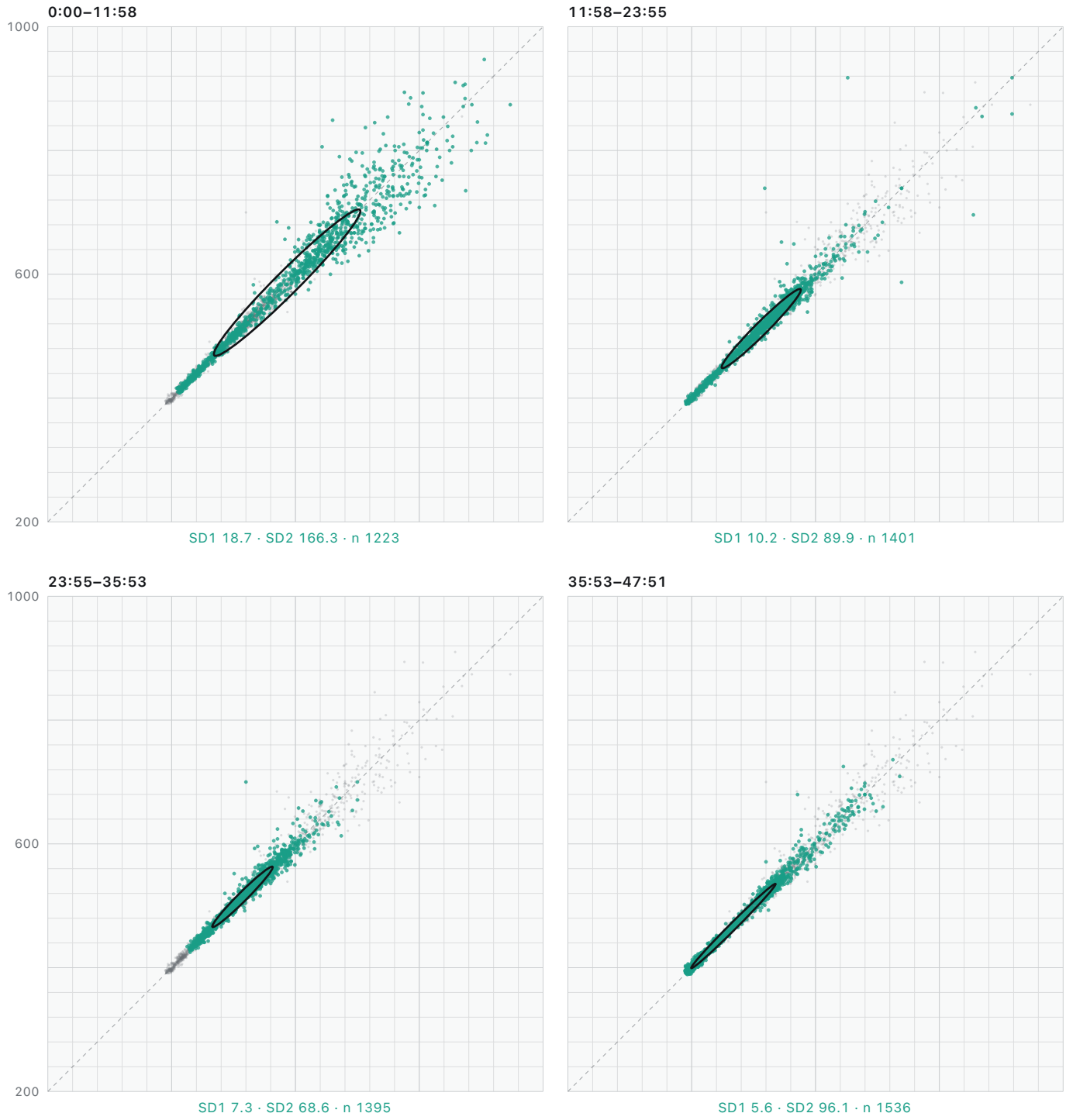


Figure 4. Poincaré plot over time: the recording split into four consecutive quarters, on a common scale, each with its own SD1/SD2 ellipse (n = intervals of the corrected series ending in the window; segments.csv gives beats_recorded and beats_analysis). Grey: the whole recording. Possible because every beat keeps its position in time.

SPECTRUM & DISTRIBUTION

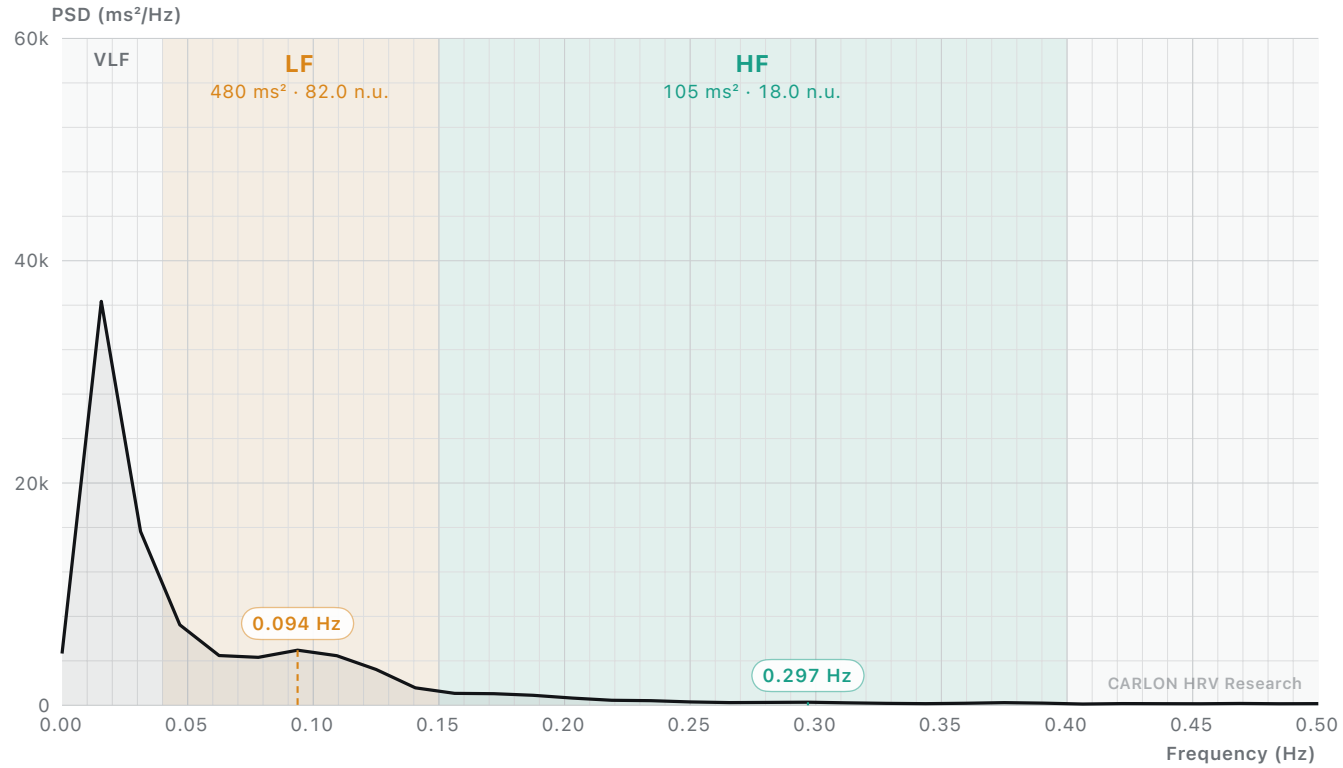


Figure 5. Power spectral density (Welch's method after cubic-spline resampling at 4 Hz). Shaded: LF 0.04–0.15 Hz and HF 0.15–0.40 Hz with absolute power, normalised units and peak frequency (dashed).

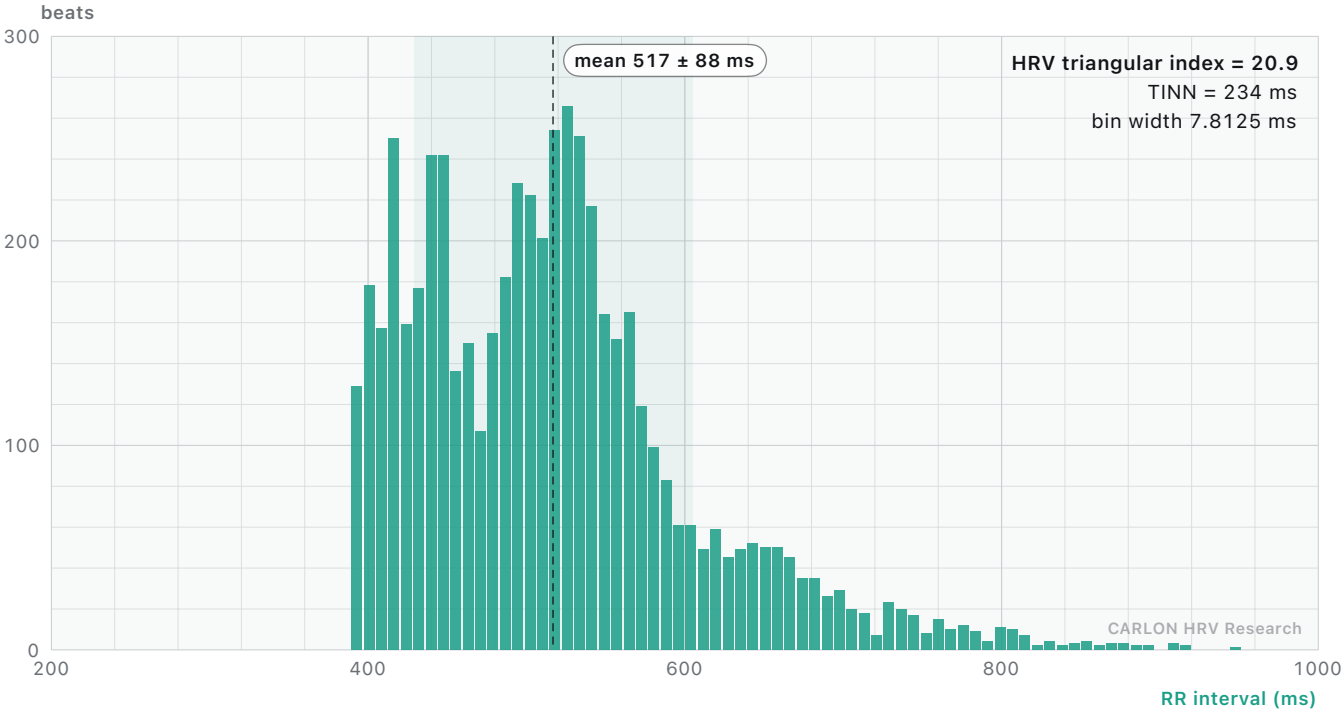


Figure 6. RR interval histogram of the corrected series, bin width 7.8125 ms (1/128 s; Task Force, 1996). Band: mean ± 1 SD. HRV triangular index = number of beats / height of the tallest bin.

SEGMENTS & EVENTS

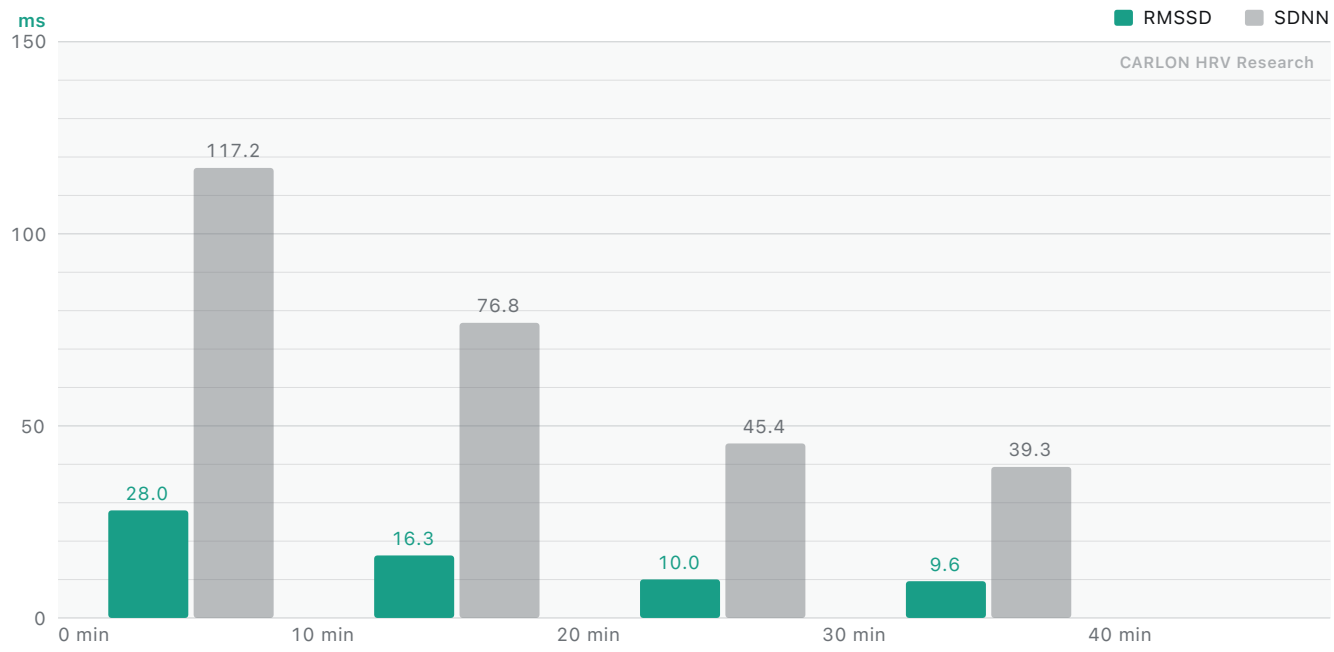


Figure 7. RMSSD and SDNN per 10-min segment of the corrected series (RR_corrected_ms × corrected_count in the CSV). With L = 10 min, segment k spans [k·L, (k+1)·L) on the beat-end time axis (Timestamp_ms): a beat belongs to the segment in which it ends. Values above the bars; an incomplete final segment is not shown.

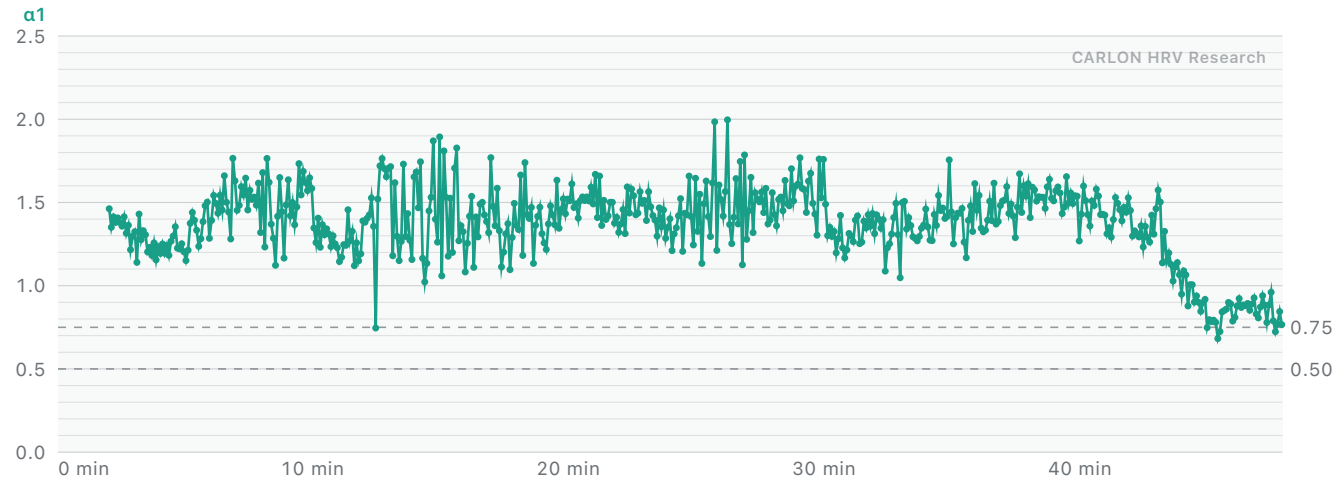


Figure 8. DFA α1 over time (Rogers et al., 2026): 120-s windows every 5 s, smoothness priors λ = 500 (Kubios default), box sizes 4–16 beats; each point at the window end. Grey ticks: windows without a valid value (5 % or more corrected beats, residual artefact, or α1 < 0). Dashed lines at 0.75 and 0.50 mark values discussed in the exercise literature, for orientation only — no thresholds are applied. Values: _dfa_alpha1.csv.

No events were marked during this recording.

METHODS — ready to use in your manuscript

RR intervals were recorded with a Polar H10 (recording path not stored with this recording; RR resolution in the data: 1 ms) and processed with CARLON HRV Research, version 1.4, build 2026102801 (Rohwedder, 2026). The recording comprises 5544 RR intervals over 2871.2 s (sum of intervals), starting 2026-10-23 17:09:00 Europe/Berlin (UTC+02:00; start time source not recorded). Beats were classified with the algorithm of Lipponen and Tarvainen (2019) (α = 5.2, 91-beat windows, c_1 = 0.13, c_2 = 0.17; implementation verified beat for beat against NeuroKit2 signal_fixpeaks), with both thresholds bounded below at 30 ms so that beat-to-beat changes smaller than 30 ms, typical of exercise, are not classified as artefacts (see the app's validation report). 0.97 % of beats were flagged. Each run of consecutive flagged intervals was replaced by equal intervals of the same total duration, their number given by whole multiples of the local rhythm where every interval of the run is one (missed beats), otherwise by the classification (one fewer per extra beat, otherwise the same, so a premature beat and its compensatory pause are averaged); normal beats were left unchanged and the duration of the recording was preserved, except for single flagged intervals without compensation, which were replaced by the mean of their neighbours. The per-beat classification and correction are included in the complete export. Mean heart rate was computed as 60 000 / mean RR over all original intervals; SDNN, RMSSD, pNN50 and the Poincaré descriptors SD1 and SD2 (Brennan et al., 2001) were computed on the corrected series. Spectral power was estimated over the whole corrected series with Welch's method (symmetric Hann window of 256 samples = 64 s, 50 % overlap, segment mean removed, density scaling) after natural cubic-spline resampling at 4 Hz; band powers were integrated exactly at the band limits (LF 0.04–0.15 Hz, HF 0.15–0.40 Hz; Task Force, 1996). Baevsky's stress index is reported as √SI with SI = AMo / (2 · Mo · MxDMn) (Baevsky, 1984): histogram of the corrected series with 50-ms bins on the absolute grid (…, 600–650, 650–700 ms …; Baevsky and Kubios convention); Mo = centre of the tallest bin (s), AMo = its share of beats (%), MxDMn = range of the series (s); from 10 min of recording the median over consecutive 5-min windows. Short-term fractal scaling (DFA α1) was computed over windows of 4–16 beats on the whole recording without prior detrending (Peng et al., 1995). Time-varying DFA α1 (Figure 8) followed Rogers et al. (2026): 120-s windows recomputed every 5 s on the corrected series after smoothness-priors detrending (Tarvainen et al., 2002; λ = 500, the Kubios default, as the review does not specify λ); windows with 5 % or more corrected beats were omitted, between the 3 % level with small bias and the 6 % level with proportional bias in Rogers et al. (2021) and in line with the exclusion criterion of Schaffarczyk et al. (2022). Segments (Figure 7) and the 60-s epochs of the data export use fixed time grids; a beat belongs to the window in which its interval ends. The RMSSD trace in Figure 1 uses a sliding window of 30 beats as a display aid only. The app's computations were validated against NeuroKit2 (331 of 331 checks passed; CARLON HRV Research validation report). Original RR intervals were retained unaltered for export.

HOW TO CITE THE SOFTWARE

Rohwedder, J. (2026). CARLON HRV Research (Version 1.4, build 2026102801) [Mobile application software]. Vitalkultur. https://vitalkultur.com/hrv-research/

LIMITATIONS OF THIS RECORDING

- No breathing record: frequency-domain values (LF, HF, LF/HF) cannot be related to breathing rate.
- Whole-recording DFA α1 averages across all phases of the recording; use the α1 time course (Figure 8) and the per-window CSV for interpretation.

PROVENANCE

Recording ID	B45E9D87-302D-4F15-8606-94A80A3F6C9F
Participant	ANON-9AD40F75 (pseudonymised)
Start	2026-10-23 17:09:00 (Europe/Berlin) · UTC+02:00
Start time source	not recorded
Beats · duration	5544 · 2871.170 s (sum of RR)
Sensor / protocol	Polar H10 · Polar H10, RR intervals at 1 ms resolution (recording path not stored with this recording)
Software	CARLON HRV Research 1.4 (2026102801)
Report generated	2026-10-29T13:51:58Z
RR series SHA-256	0dc665e19322c11292800b93bf4a6770c466c16e9cac6bfb4a472eeb3c6f58c4
Audit trail at report time	event 1 · 98e6a500fb67d050098a62a77f9818e951ddf853888799a240fa14f60f81ed62

SHA-256 recipe: UTF-8 bytes of the RR intervals rounded to 0.1 ms half away from zero (floor(x·10 + 0.5)/10), formatted with one decimal and '.', joined by ','. The audit-trail hash links this report to the hash chain in the JSON of the same export.

REFERENCES

Baevsky RM, Kirillov OI, Kletskin SZ (1984). Mathematical analysis of heart rate changes under stress. Moscow: Nauka.

Brennan M, Palaniswami M, Kamen P (2001). Do existing measures of Poincaré plot geometry reflect nonlinear features of heart rate variability? IEEE Trans Biomed Eng 48(11):1342–1347.

Lipponen JA, Tarvainen MP (2019). A robust algorithm for heart rate variability time series artefact correction using novel beat classification. J Med Eng Technol 43(3):173–181.

Makowski D, Pham T, Lau ZJ, Brammer JC, Lespinasse F, Pham H, Schölzel C, Chen SHA (2021). NeuroKit2: A Python toolbox for neurophysiological signal processing. Behav Res Methods 53:1689–1696.

Peng CK, Havlin S, Stanley HE, Goldberger AL (1995). Quantification of scaling exponents and crossover phenomena in nonstationary heartbeat time series. Chaos 5(1):82–87.

Rogers B, Giles D, Draper N, Mourot L, Gronwald T (2021). Influence of artefact correction and recording device type on the practical application of a non-linear heart rate variability biomarker for aerobic threshold determination. Sensors 21(3):821.

Rogers B, Fleitas-Paniagua PR, Murias JM (2026). Heart rate variability DFA a1: from lab to consumer exercise prescription. Exerc Sport Sci Rev. doi:10.1249/JES.0000000000000401

Schaffarczyk M, Rogers B, Reer R, Gronwald T (2022). Validity of the Polar H10 sensor for heart rate variability analysis during resting state and incremental exercise in recreational men and women. Sensors 22(17):6536.

Task Force of the European Society of Cardiology and the North American Society of Pacing and Electrophysiology (1996). Heart rate variability: standards of measurement, physiological interpretation and clinical use. Circulation 93(5):1043–1065.

Tarvainen MP, Ranta-aho PO, Karjalainen PA (2002). An advanced detrending method with application to HRV analysis. IEEE Trans Biomed Eng 49(2):172–175.

Welch PD (1967). The use of fast Fourier transform for the estimation of power spectra: a method based on time averaging over short, modified periodograms. IEEE Trans Audio Electroacoust 15(2):70–73.

Software and documentation

CARLON HRV Research 1.4 (2026102801) · https://vitalkultur.com/hrv-research/. Research tool, not a medical device; values are not diagnostic.